Pergamon

Solid State Communications, Vol. 105, No. 3, pp. 145–149, 1998

Printed in Great Britain
0038–1098/98 $19.00+.00

PII: S0038–1098(97)10078-3

ELECTRON DIFFRACTION STUDY OF SINGLE-WALL CARBON NANOTUBES

D. Bernaerts,[a,*] A. Zettl,[b] Nasreen G. Chopra,[b] A. Thess[c] and R.E. Smalley[c]

[a]National Center for Electron Microscopy, Lawrence Berkeley National Laboratory, Berkeley, CA 94720, U.S.A.
[b]Department of Physics, University of California at Berkeley and Materials Sciences Division, Lawrence Berkeley National Laboratory, Berkeley, CA 94720, U.S.A.
[c]Center for Nanoscale Science and Technology, Rice Quantum Institute and Departments of Chemistry and Physics, MS-100, Rice University, P.O. Box 1892, Houston, TX 77251, U.S.A.

(*Received* 16 *July* 1997; *accepted* 16 *October* 1997 *by S.G. Louie*)

We have used selected-area electron diffraction techniques to investigate the structure of single-wall carbon nanotubes assembled into ropes. The diffraction is sensitive to details of the tube curvature, orientation, radius and chirality. Single-wall carbon nanotubes within the ropes are found to comprise largely tubes of armchair chirality, but not exclusively (10, 10) tubes. © 1997 Published by Elsevier Science Ltd

1. INTRODUCTION

Carbon nanotubes [1] have attracted much interest in recent years. Theoretical calculations on these cylindrical all-carbon structures predict a strong dependence of the electrical properties on the detailed geometrical structure of the nanotubes [2, 3]. For example, a small change in diameter, accompanied by a change in chiral angle, can be sufficient to transform a metallic nanotube into a non-metallic one. Therefore, production methods which enable the tuning of both radius and chiral angle, or are at least selective for specific classes of nanotube geometries, are desirable for both fundamental studies and applications of nanotubes. Similarly, complementary observation techniques able to distinguish between different types of nanotubes are essential for complete characterization of the nanotube structures.

Transmission electron microscopy techniques have been successfully used to characterize the structure of both single [4–6] and multiwalled carbon nanotubes (e.g. [1, 7, 8]). The measurement of the electrical properties of individual carbon nanotubes is difficult due to the extremely small size of the nanotubes [9, 10] and is ideally performed on tubes that have been structurally fully characterized. Experimental confirmation of the dependence of the electrical properties of the nanotubes on their detailed structure is ideally performed on high purity samples of single shell nanotubes. Multishell nanotubes in general contain layers with different chirality making the correspondence between geometrical and electrical properties exceedingly difficult to examine.

Recently, a two-laser ablation method using a target of graphite mixed with magnetic catalyst has been successfully employed to produce single wall nanotubes in high yields [11]. The single wall nanotubes thus produced are almost exclusive assembled into bundles or ropes containing of order 100 tubes each; within the rope the individual tubes are parallel to one another, held in place by weak intertube interactions, presumably of the van der Waals form. Transmission electron microscopy images and X-ray diffraction patterns of the rope material suggest a high uniformity in individual tube diameter of approximately 13 Å. Electrical conductivity measurements on bulk rope samples have revealed a metallic behavior, consistent with the predicted electronic structure of individual (10, 10) tubes. Using these observations as a basis, it has been argued that the majority of the nanotubes in the ropes are (10, 10) nanotubes.

In this Communication, we present results of selected-area electron diffraction studies performed on isolated ropes of single wall carbon nanotubes. Our measurements are sensitive to not only the diameter but also the chirality of the individual nanotubes comprising the rope. Since electron diffraction is able to reveal the

*Present address: EMAT, University of Antwerp RUCA, Groenenborgerlaan 171, B2020 Antwerp, Belgium.

hk.0 reflections and their orientation with respect to the tube axis, this method is well suited to determine in a more direct way the geometrical details of single wall nanotubes contained in rope specimens [1, 4, 7]. We find that single wall nanotubes comprising ropes have a narrow diameter distribution peaked at 13 Å, consistent with previous findings, but that the tubes are not exclusively of the (10, 10) variety. Instead, there is a mixture of tube chiralities within a given rope.

2. EXPERIMENTAL

Ropes of single wall carbon nanotubes were produced at Rice University by the double laser ablation method as described in [11]. The tube material was then mechanically transferred to a copper transmission electron microscope (TEM) grid; it is possible that some ropes were bent and twisted by this mechanical handling of the sample. The grid with attached nanotube rope samples was then examined in a JEOL 200 CX transmission electron microscope at the National Center for Electron Microscopy at the Lawrence Berkeley National Laboratory. Care was taken to avoid radiation damage of the tubes due to the 200 keV electron beam by limiting exposure.

Real-space TEM images of the rope specimens generally agreed well with images previously reported [11]. Effective "cross-sections" of the ropes (with tube axes perpendicular to the image plane) displayed a close-packed triangular arrangement of the tubes, although this triangular arrangement seemed to be perfect only over lengths of some hundreds of nanometers along the tube length. Bending and twisting of the complete rope (and possibly shifting of nanotubes inside the ropes) disturbs the triangular arrangement over longer distances. Figure 1

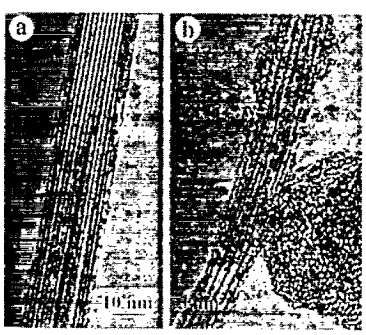

Fig. 1. Real-space TEM images of ropes of single wall carbon nanotubes, with a parallel close-packing arrangement of the tubes within the rope. (a) A straight, untwisted region of the rope. Such "ideal" regions are observed only over relatively small distances along the rope. (b) A visibly bent and twisted region of the rope. Twisting of the ropes and shifting of the tubes within the rope disorders the ideal parallel triangular stacking.

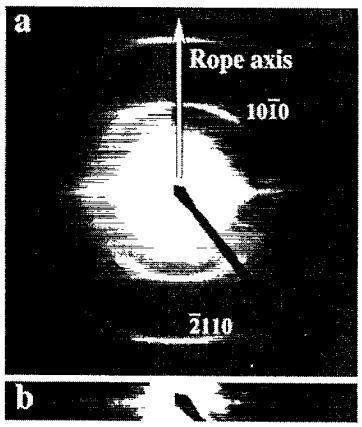

Fig. 2. Experimental selected area electron diffraction pattern of a rope of single wall carbon nanotubes. (a) Large area of reciprocal space. The *hk*.0 reflections are diffuse arcs and, although difficult to see in this image, the radial reflections (normal to rope axis) show sharp reflections due to the triangular stacking of the tubes in the rope. (b) Detail near origin of the radial reflections of the same rope as in (a), but obtained with a shorter exposure time. The spots due to the triangular stacking of the tubes within the rope are clearly resolved.

shows examples of such behavior in real-space TEM images, where here the tubes axes lie in the image plane. Figure 1(a) shows a straight rope region where the individual nanotubes are in excellent alignment with no twisting or bending of the rope. Figure 1(b) shows a section of rope that displays obvious bending and twisting of the nanotubes.

Since the large majority of the nanotubes are arranged in ropes and due to the relatively large size of the selected area aperture, we were not able to obtain diffraction patterns of isolated single walled tubes. However, diffraction patterns of isolated ropes were readily obtained and care was taken to select ropes which appeared to be straight (i.e. straight at least in projection along the direction of the electron beam) and which had a constant diameter.

Figure 2(a) shows a typical rope diffraction pattern obtained in the TEM. A row of reflections, through the origin and perpendicular to the rope axis, is the most prominent feature visible in the diffraction pattern. Figure 2(b) shows the origin region in greater detail; the horizontal streak through the origin is composed of a series of well-defined spots. Figure 2(a) shows also much weaker diffuse circles around the central spot, with streaks originating from these circles and continuing outward in a direction perpendicular to the rope axis. In none of the observed diffraction patterns could sharp reflections, except for the ones on the line through the origin and perpendicular to the rope axis [Fig. 2(b)], be observed. The diffracted intensity in the diffuse rings is not uniform over the complete ring, indicating that it is

not caused by amorphous material which is possibly present on the rope surface.

3. DISCUSSION

It has been suggested that the dual laser ablation method favors the growth of single walled carbon nanotubes with indices, using the conventional nanotube notation, of (10, 10). In order to determine if the experimentally observed diffraction patterns are fully consistent with (10, 10) nanotubes, we discuss the expected diffraction pattern of a single perfect (10, 10) tube and a perfect crystalline rope of aligned (10, 10) tubes. Discrepancies between the predicted and observed patterns lead us to consider the diffraction patterns expected from "imperfect" ropes, i.e. ropes consisting of non-parallel tubes or tubes other than (10, 10).

In the literature at least two methods have been reported to model the electron diffraction pattern for a specific carbon nanotube. One possibility is to use the geometrical reciprocal space model described by Zhang *et al.* [7], which gives information about the position of the *hk*.0 reflections as a function of tilting of the nanotubes with respect to the electron beam. Qin [12] and Lucas *et al.* [13] calculated diffraction intensities for carbon nanotubes based on the kinematical approximation for electron diffraction. The calculated positions of the spots agree well with the positions obtained from the geometrical model, but additionally information about the broadening of the reflections due to the curvature of the graphene sheet and about the intensity distribution along the streaks can be obtained.

Figure 3(a) shows for normal incidence (i.e. electron beam perpendicular to the tube axis) the predicted diffraction pattern of an isolated (10, 10) carbon nanotube from the geometrical model [7]. In this orientation there is one set of carbon–carbon bonds perpendicular to the tube axis. One therefore obtains a hexagonal set of *hk*.0 reflections with the 0 1 $\bar{1}$ 0 reflection perpendicular to the tube axis. The reflections are streaked along directions perpendicular to the tube axis and away from it. For this isolated single-tube model, the central spot is streaked in the same direction.

For a rope of triangularly stacked parallel (10, 10) tubes one again expects distinct *hk*.0 reflections as for the isolated (10, 10) tube; indeed only the diffraction intensity along the line through the central spot and perpendicular to the rope axis will change. Depending on the orientation of the triangular lattice of the tubes with respect to the electron beam, one obtains different discrete spots at the positions where Ewald's sphere intersects the loci of the reciprocal lattice of this triangular tube arrangement. We do not show these spots in our diffraction simulations of Fig. 3, but they

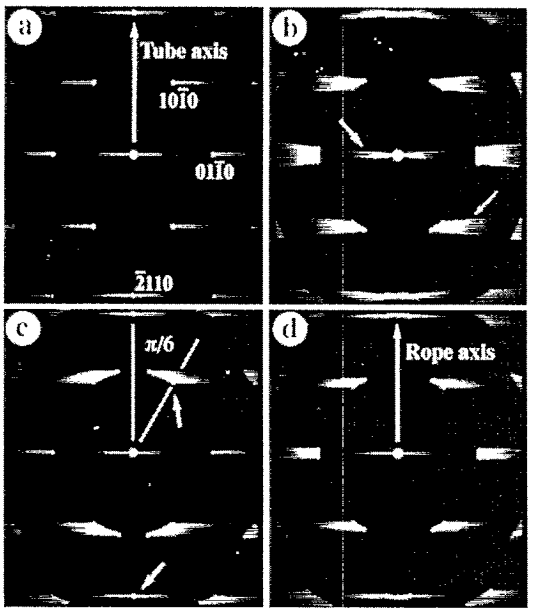

Fig. 3. Simulated electron diffraction patterns for (a) an isolated single wall (10, 10) carbon nanotube and (b–d) for "imperfect" ropes of nanotubes. (b) assumes a model where the (10, 10) tubes are all in normal incidence, but not parallel in the plane normal to the electron beam. (c) assumes a model where the (10, 10) tubes are not all in normal incidence, but all tubes are parallel in projection along the direction of the electron beam. (d) assumes a model of parallel tubes, but with a distribution of chiral angles. Small arrows highlight differences with experimental data (see text). The simulation (d) is most consistent with the experimental diffraction pattern of Fig. 2, indicating that the ropes are not composed exclusively of (10, 10) tubes.

can clearly be observed in the experimental data for the real rope in Fig. 2(b). The experimentally obtained horizontal diffraction streak with well-defined spots near the origin [Fig. 2(b)] is thus consistent with the above model predictions.

We now turn to the origin of the diffuse arcs observed experimentally [Fig. 2(a)]. There exist several possibilities for the observation of these diffuse arcs. According to the analytical calculations [12, 13], the diffraction intensity is restricted to a few discrete lines perpendicular to the tube axis: the so-called layerlines. This shows that the reflections cannot be broadened (due to the strong curvature of the graphene structure) in the direction parallel to the tube axis. Along a layerline, the diffraction intensity is essentially given by a series of Bessel functions, thus leading to broadening of the spots along the layerlines and to intensity variations in the streaks. The strong curvature of the graphene structure in the (10, 10) tubes (which was held responsible for the absence of the *hk*.0 reflections in the X-ray patterns [11]) can thus not be an explanation for the observation of the

diffuse arcs in the experimental diffraction patterns and a perfect rope consisting purely of (10, 10) nanotubes cannot cause the observed electron diffraction patterns.

We first consider the case of an imperfect rope formed exclusively from (10, 10) single walled nanotubes but with geometrical shifts of the tubes within the rope and twists of the entire rope. The effect of this twisting and shifting on the electron diffraction patterns can be estimated by considering the diffraction patterns of a set of non-parallel (10, 10) tubes. Two extreme cases are here considered: (i) all nanotubes are perpendicular to the electron beam, but are rotated with respect to each other in planes normal to the electron beam and (ii) all nanotubes are parallel in projection along the electron beam, but are rotated with respect to each other in planes parallel to the electron beam.

For the case (i), all nanotubes axes are normal to the electron beam and the resulting diffraction pattern is a superposition of patterns such as those of Fig. 3(a) but rotated about the central spot. Figure 3(b) shows a schematic representation of the resulting pattern. All spots, including those near the origin, become diffuse arcs, but the streaks are not parallel to each other. The rotation of the tubes results in a tell-tale diffraction signature: diffuse arcs or wings surround the origin and there is no longer a sharp streak or line of radial reflections through the central spot. Although electron diffraction patterns of the type just described [Fig. 3(b)] were observed for bent ropes, ropes with no obvious bending displayed patterns only such as shown in Fig. 2, with sharp radial reflections through the central spot. Hence we rule out the form of disorder of case (i) as the origin of the experimentally observed diffuse arcs surrounding the higher order diffraction peaks of Fig. 2(a).

For disorder case (ii), one has to consider the diffraction patterns for inclined incidence of the electron beam [7]. Each *hk*.0 locus is in fact a circle in the 3-dimensional reciprocal space of the nanotube, centered on the tube axis and perpendicular to it. For inclined incidence, Ewald's plane intersects these circles above or below the line through their center and as a consequence, upon tilting, the refections move away from the line containing the radial reflections and simultaneously move towards the tubule axis [7]. A superposition of such diffraction patterns leads to a pattern such as shown schematically in Fig. 3(c). The line of radial reflections remains sharp and most other reflections become diffuse arcs and all streaks are parallel. However, for a (10, 10) tube, the maximum angle between the tube (rope) axis and the edge of the $1\ 0\ \bar{1}\ 0$ arc is $\pi/6$, i.e. the position of the $1\ 0\ \bar{1}\ 0$ reflection for normal incidence. Furthermore, the $2\ \bar{1}\ \bar{1}\ 0$ reflection is only visible for normal incidence: the $2\ \bar{1}\ \bar{1}\ 0$ locus is in fact a circle with zero radius on the tube axis and can only be intersected by Ewald's sphere if the electron beam is normal to the tube axis. However, in the experimental electron diffraction pattern of Fig. 2(a), the $1\ 0\ \bar{1}\ 0$ arc extends further than $\pi/6$ and the $2\ \bar{1}\ \bar{1}\ 0$ reflection is clearly an arc. Hence, the form of disorder of case (ii) is again insufficient to account for the experimental diffraction data.

In reality, real tube rotational disorder within a rope of carbon nanotubes is a combination of the two extreme cases (i) and (ii), but even a combination of these rotational disorder types is unable to account for the experimentally observed diffuse arcs. It is thus impossible to explain the observed electron diffraction patterns in terms of imperfect ropes of (10, 10) tubes.

We now turn to the possibility that disorder in the ropes comes from incorporation of non-(10, 10) tubes. We find that ropes consisting of parallel tubes with a distribution in chirality can in fact explain the features observed in the electron diffraction patterns. The radial reflections remain sharp, streaks are parallel and most reflections become diffuse arcs with no limitations on their angular extent (i.e. if one considers a large number of tubes with different chiral angle and the above described effects blurring the discrete spots into continuous arcs).

Figure 3(d) shows a simulated diffraction pattern for a rope of parallel single walled tubes with a distribution of chiral angles. Tubes with chiral angles of at least 10° (due to the unknown orientation of the rope axis with respect to the electron beam; this is only a lower limit) with respect to the armchair structure of a (10, 10) nanotube are required to cause the bright *hk*.0 arcs of the experimentally observed patterns. This is still consistent with a reasonable uniformity in diameter of the tubes: as many as six different tubes can be found in the 13.4–13.8 Å diameter range, four of them having chiral angles less than 10° deviating from the armchair configuration.

However, the fact that the experimentally determined bright arcs as in Fig. 2(a) are terminated at a certain angle indicates that not all chiral angles are present in the ropes. The large majority of the tubes have a structure relatively close to the armchair configuration. The number of zigzag nanotubes (or tubes with a structure close to the zigzag configuration) present in the ropes is too small to be detectable by the selected area electron diffraction measurements discussed here.

4. CONCLUSION

Selected area electron diffraction patterns of ropes of single wall carbon nanotubes show that the ropes do not contain exclusively (10, 10) nanotubes. The observed patterns can only be explained by assuming a distribution

of chiral angles. However, the majority of the nanotubes are found to be close to the armchair-structure of (10, 10) nanotubes and zigzag-type tubes or chiral tubes with structures close to the zigzag configuration can only be present in very small numbers. This indicates that the two-laser growth process for single wall nanotubes favors armchair-like structures [11].

The fact that the ropes do not consist purely of metallic (10, 10) nanotubes has important consequences for the interpretation of a variety of experiments being carried out on such samples, including electrical, thermal, optical and mechanical measurements [14, 15].

Acknowledgements—We thank Dr. U. Dahmen for making the facilities of the National Center for Electron Microscopy, Lawrence Berkeley National Laboratory, available to this project. This research was supported in part by a UC Berkeley Chancellor's Initiative Grant (AZ), the National Science Foundation (AZ, RES), the U.S. Department of Energy (AZ), the Office of Naval Research (AZ) and the Texas Advanced Technology Program (RES). AZ received support from the Miller Institute for Basic Research in Science.

Note added: After the completion of this work, we became aware of unpublished experiments performed simultaneously by Cowley *et al.* [16] using nanoprobe electron diffraction on similar carbon nanotube samples. Results obtained by Cowley *et al.* are consistent with the findings presented here.

REFERENCES

1. Iijima, S., *Nature*, **354,** 1991, 56.
2. Hamada, N., Sawada, S.-I. and Oshiyama, A., *Phys. Rev. Lett.*, **68,** 1992, 1579.
3. Dresselhaus, M.S., Dresselhaus, G. and Saito, R., *Solid State Commun.*, **84,** 1992, 201; Saito, R., Fujita, M., Dresselhaus, G. and Dresselhaus, M.S., *Appl. Phys. Lett.*, **60,** 1992, 2204.
4. Iijima, S. and Ichihashi, T., *Nature*, **363,** 1993, 603.
5. Bethune, D.S., Kiang, C.H., de Vries, M.S., Gorman, G., Savoy, R., Vazquez, J. and Beyers, R., *Nature*, **363,** 1993, 605.
6. Ajayan, P.M., Lambert, J.M., Bernier, P., Barbedette, L., Colliex, C. and Planeix, J.M., *Chem. Phys. Lett.*, **215,** 1993, 509.
7. Zhang, X.F., Zhang, X.B., Van Tendeloo, G., Amelinckx, S., Op de Beeck, M. and Van Landuyt, J., *J. Cryst. Growth*, **130,** 1993, 368; Zhang, X.B., Zhang, X.F., Amelinckx, S., Van Tendeloo, G. and Van Landuyt, J., *Ultramicroscopy*, **54,** 1994, 237.
8. Ajayan, P.M., Ichihashi, T. and Iijima, S., *Chem. Phys. Lett.*, **202,** 1993, 384.
9. Langer, L., Stockman, L., Heremans, J.P., Bayot, V., Olk, C.H., Van Haesendonck, C., Bruynserade, Y. and Issi, J.-P., *J. Mater. Res.*, **9,** 1994.
10. Ebbesen, T.W., Lezec, H.J., Hiura, H., Bennett, J.W., Ghaeme, H.F. and Thio, T., *Nature*, **382,** 1996, 54.
11. Thess, A., Lee, R., Nikolaev, P., Dai, H., Petit, P., Robert, J., Xu, C., Lee, Y.H., Kim, S.G., Colbert, D.T., Scuseria, G., Tomanek, D., Fisher, J.E. and Smalley, R.E., *Science*, **273,** 1996, 483.
12. Qin, L.C., *J. Mater. Res.*, **9,** 1994, 2450.
13. Lucas, A.A., Bruyninckx, V., Lambin, Ph., Bernaerts, D., Amelinckx, S., Van Landuyt, J. and Van Tendeloo, G., Submitted for publication.
14. Bockrath, M., Cobden, D.H., McEuen, P.L., Chopra, N.G., Zettl, A., Thess, A. and Smalley, R.E., *Science*, **275,** 1997, 1922.
15. Tans, S.J. *et al.*, *Nature*, **386,** 1997, 474.
16. Cowley, J.M., Nikolaev, P., Thess, A. and Smalley, R.E., Submitted for publication.